

# Relations between MaxRotD50 and some horizontal components of ground motion intensity used in practice

Alan Poulos\*<sup>1</sup> and Eduardo Miranda<sup>1</sup>

<sup>1</sup>Department of Civil and Environmental Engineering, Stanford University,  
473 Via Ortega, Stanford, California 94305, U.S.A.

## Abstract

The most commonly used intensity measure of ground motion in earthquake engineering is the 5%-damped spectral ordinate, which varies in different directions. Several different measures have been proposed over the years to combine the intensity of the two horizontal recorded ground motions to derive ground-motion models as well as for design purposes. This study provides the relation to seven previously used measures of horizontal ground motion with respect to a recently proposed orientation-independent measure of horizontal ground motion intensity referred to as MaxRotD50. This new measure of horizontal intensity is defined as the median value of the maximum spectral ordinate of two orthogonal directions computed for all possible non-redundant orientations. The relations are computed using 5,065 pairs of horizontal ground motions taken from the database of ground motions recorded in shallow crustal earthquakes in active tectonic regions developed as part of the Pacific Earthquake Engineering Research Center–Next Generation Attenuation–West2 project. Empirically-derived period-dependent relations are presented for three quantities which permit transforming any of the seven other definitions of horizontal ground motion intensity to MaxRotD50, namely: (1) geometric mean of the ratio of MaxRotD50 to any of the seven other measures of intensities; (2) standard deviation of the natural logarithm of the ratio of MaxRotD50 to any of the seven other measures of intensities; and (3) the correlation between the natural logarithm of the ratio of MaxRotD50 to the other measures of intensities and the natural logarithm of the other measure of intensity. Additionally, the influence of site-class at the recording station, earthquake magnitude, and distance to the horizontal projection of the rupture is examined on the geometric mean of the ratio of MaxRotD50 to the median intensity of all non-redundant orientations (i.e., RotD50), showing negligible influence of site class and only a relatively small influence of magnitude and distance.

---

\*Corresponding author: apoulos@stanford.edu

## INTRODUCTION

Earthquake shaking has two horizontal components of ground motion, which are usually recorded in orthogonal directions. Although some methods have been proposed to consider the orientation dependence of ground motion intensity (e.g., [Hong and Goda, 2007](#)), usually a single measure of intensity is used to characterize horizontal ground motions. In most cases, 5%-damped response spectral ordinates are used as measures of ground motion intensity, such as for the development of ground motion models (GMMs) and to define target spectra for earthquake-resistant design. Several methods have been used to combine measures of intensity of both recordings into a single ground motion intensity. The simplest options consist of combining the intensities of the two as-recorded directions, such as by taking the geometric mean intensity, which was usually used in early GMMs (e.g., [Youngs et al., 1988](#); [Abrahamson and Silva, 1997](#); [Sadigh et al., 1997](#)), choosing one of the directions at random (e.g., [Boore et al., 1997](#); [Atkinson and Boore, 2003](#)), or using the largest of the two intensities, as done by the ShakeMap project ([Worden et al., 2020](#)). Another option is to compute the intensity in a direction that relates to the orientation with respect to the seismic source, such as using the fault-normal or fault-parallel directions ([Somerville et al., 1997](#)). Lastly, definitions of horizontal intensity that do not depend on the geometry of the source nor the orientation of the horizontal orthogonal sensors have also been proposed, which are computed using the geometric mean of all non-redundant orientation angles of the two orthogonal horizontal components and then finding the geometric mean corresponding to a certain percentile of the resulting set of geometric means ([Boore et al., 2006](#)). One of these definitions was used in the GMMs of the Pacific Earthquake Engineering Research (PEER) center's Next Generation Attenuation of Ground Motions (NGA) project (e.g., [Boore and Atkinson, 2008](#); [Campbell and Bozorgnia, 2008](#); [Chiou and Youngs, 2008](#)). [Boore \(2010\)](#) introduced a measure of ground motion horizontal-component intensity that does not require the computation of the geometric mean of two orthogonal components and is still independent of the in situ orientations of the recorded ground motion. His proposed measure of intensity, referred to as RotDpp is computed by calculating the 5% damped spectral ordinate for all non-redundant rotations of the two recorded horizontal components of a ground motion (i.e., for a range of azimuths from  $0^\circ$  to one rotation-angle increment less than  $180^\circ$  because a spectral ordinate is by definition the peak value of the absolute value of the response of the oscillator and therefore it has a rotation-angle periodicity of  $180^\circ$ ) and then finding a certain percentile pp of the set of spectral ordinates. The NGA-West2 project used RotD50 as a measure of horizontal ground motion intensity and some of the latest GMMs used this parameter (e.g., [Boore et al., 2014](#)).

Several studies have derived empirical relations between different definitions of the horizontal ground motion intensity (e.g., [Beyer and Bommer, 2006](#); [Watson-Lamprey and Boore, 2007](#); [Huang et al., 2008](#); [Shahi and Baker, 2014](#); [Boore and Kishida, 2017](#)). These relations can be used to convert one definition to another, which is useful for example in probabilistic seismic hazard analysis (PSHA) when combining GMMs derived using different definitions of horizontal component.

On the other hand, because of their overall geometry in plan and the arrangement of their lateral-load-resisting elements, most structures have two horizontal principal axes that are orthogonal to each other. The design of most structures to resist seismic loading is typically done by conducting either static or response spectrum modal analyses where the same horizontal design spectrum is applied to the two horizontal principal axes of the structure. Therefore, of particular interest to structural engineers is the probability that the ground motion will exceed the design intensity in at least one of these two orthogonal horizontal principal axes of the structure. Since the orientation of

the ground motion with respect to the principal directions of the building is unknown, the maximum intensity of the two directions can be computed at different orientations. In order to use a measure of ground motion intensity that is conceptually more relevant to the design of structures, [Poulos and Miranda \(2022\)](#) recently proposed a new measure of horizontal ground motion intensity that is also independent of the in situ orientations of the horizontal recording sensors. The new measure of horizontal ground motion intensity is computed as the largest spectral ordinate of two orthogonal directions of all non-redundant angles (for a range of azimuths from  $0^\circ$  to one rotation-angle increment less than  $90^\circ$ ) and then computing the 50th percentile (i.e., the median) of the set of spectral ordinates. Following the notation introduced by [Boore et al. \(2006\)](#), the new measure of ground motion intensity is referred to as MaxRotD50, where the prefix Max refers to the selection of the maximum of two orthogonal horizontal pseudo-acceleration spectral ordinates. This definition has the advantage that, if the orientation of the ground motion with respect to the principal directions of the structure is assumed to be uniformly distributed, the probability that MaxRotD50 will be exceeded in at least one of the principal directions of the structure is, by definition, 50%, whereas the equivalent probability of exceeding RotD50 in at least one of the two principal directions of the structure varies from record to record but is significantly higher, being on average approximately 95% ([Poulos and Miranda, 2022](#)). Even though this measure of ground motion intensity is of greater interest to structural engineers than previously used measures, the use of MaxRotD50 is still limited at present since currently there is no GMM developed for this definition of ground motion intensity, and its relation to other horizontal components of ground motion intensity has not been studied.

This study provides relations between MaxRotD50 and several other definitions of the horizontal component of ground motions that are commonly used. These relations can be used together with existing GMMs to obtain the logarithmic mean and standard deviation of MaxRotD50 required for conducting PSHA. The relations are obtained empirically from a large dataset of ground motions from shallow crustal earthquakes in active tectonic regimes ([Ancheta et al., 2014](#)). The theoretical boundaries of the ratios are also derived.

## HORIZONTAL COMPONENTS OF GROUND MOTION

Horizontal ground motion intensity is dependent on orientation. For example, Figure 1a shows a hodogram of the relative displacement of a 5%-damped linear elastic oscillator of period 1 s subjected to both horizontal components of ground motion from the 1994 Mw 6.7 Northridge earthquake recorded at the Canoga Park station. The directions where the ground motion was recorded correspond to  $0^\circ$  and  $90^\circ$  rotation angle in the figure. The response was then used to obtain spectral acceleration ( $S_a$ ) at all rotation angles  $\theta$ , which, for a particular orientation, corresponds to the maximum of the hodogram projected onto that orientation. The result is shown in Figure 1a in a polar representation (i.e., the spectral acceleration is given by the distance between the curve and the origin), and in Figure 1b as a function of the rotation angle with respect to the orientation of the sensors installed in this recording station. The spectral accelerations in Figure 1b are only presented in a rotation angle range of  $180^\circ$  since they repeat for the next  $180^\circ$ . The orientation dependence of spectral acceleration is significant in this case since the response is fairly polarized. The degree of this dependence changes from record to record and with the period of the oscillator, but on average, the intensity in the direction of maximum intensity is approximately 39% higher and 68% higher

than the intensity in the orthogonal directions for periods of 0.1 s and 3 s, respectively (Hong and Goda, 2007). In other words, the change in intensity with change in direction is by no means small.

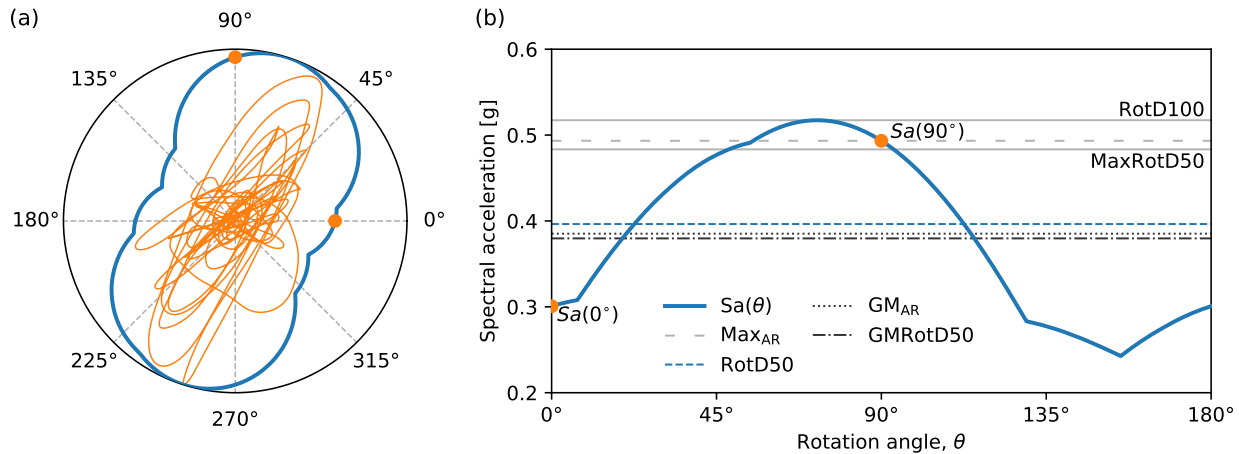


**Figure 1:** Orientation dependence of spectral acceleration for an example ground motion record shown in (a) polar and (b) linear representations.

Several methods can be used to transform the orientation-dependent representation of horizontal ground motion intensity shown in Figure 1a into a single intensity measure. The eight definitions that will be used in this study are described in Table 1 and are shown in Figure 1b for the example ground motion. The first three definitions are the simplest since they use the as-recorded orientations directly, and hence depend on the orientation of the horizontal sensors.  $GM_{AR}$  is computed by taking the geometric mean of the intensities of the as-recorded orientations and has been commonly used in several GMMs (e.g., Youngs et al., 1988; Abrahamson and Silva, 1997; Sadigh et al., 1997). Similarly,  $Max_{AR}$  is the maximum intensity in the two as-recorded orientations. The third definition corresponds to the intensity of a component arbitrarily selected from the two as-recorded components. GMMs with this definition usually use both components independently in their calibration (e.g., Boore et al., 1997; Atkinson and Boore, 2003), which results in the same logarithmic mean as would be obtained by using the geometric mean but with a higher logarithmic standard deviation (Boore et al., 1997).

The next five definitions shown in Table 1 are independent of the orientation of the sensor and require computing the intensity at all non-redundant orientations. Boore et al. (2006) introduced orientation-independent definitions that correspond to a percentile from the distribution of the geometric mean of two orthogonal horizontal components at all non-redundant orientations. The median value of this definition is termed  $GMRotD50$ . Moreover, Boore et al. (2006) also introduced  $GMRotI50$ , which corresponds to the geometric mean of two orthogonal horizontal components at a rotation angle that minimizes the difference to  $GMRotD50$  over a certain period range. Thus,  $GMRotI50$  is the only definition of Table 1 that depends on the response of oscillators with periods different from the period of interest.  $GMRotI50$  was used by the GMMs of the NGA project (e.g., Boore and Atkinson, 2008; Campbell and Bozorgnia, 2008; Chiou and Youngs, 2008). Boore (2010) then introduced another orientation-independent definition that uses a single component instead of the geometric mean of two orthogonal components. The notation of this definition is  $RotDpp$ , which corresponds to the  $pp$ -th percentile of the intensity from all orientations. Thus, the

**Table 1:** Definitions of the horizontal components of ground motion intensity used in this study.

Symbol	OI*	Definition
$GM_{AR}$	✗	Geometric mean of the as-recorded directions: $\sqrt{Sa(0^\circ)Sa(90^\circ)}$
$Max_{AR}$	✗	Maximum of the as-recorded directions: $\max\{Sa(0^\circ), Sa(90^\circ)\}$
Arbitrary	✗	$Sa(0^\circ)$ or $Sa(90^\circ)$
$GMRotD50$	✓	Median of $\sqrt{Sa(\theta)Sa(90^\circ + \theta)}$ for $\theta \in [0^\circ, 90^\circ]$
$GMRotI50$	✓	$\sqrt{Sa(\theta^*)Sa(90^\circ + \theta^*)}$ , where $\theta^*$ minimizes the difference to $GMRotD50$ over all $T$
$RotD100$	✓	Maximum $Sa$ over all rotations angles : $\max_{\theta \in [0^\circ, 180^\circ]} Sa(\theta)$
$RotD50$	✓	Median of $Sa(\theta)$ for $\theta \in [0^\circ, 180^\circ]$
$MaxRotD50$	✓	Median of $\max\{Sa(\theta), Sa(90^\circ + \theta)\}$ for $\theta \in [0^\circ, 90^\circ]$

\* Indicates if the definition is orientation independent (check mark) or orientation dependent (cross mark).

maximum intensity from all orientations is termed  $RotD100$ , which, for the example ground motion of Figure 1, occurs at a rotation angle of approximately  $73^\circ$ . Moreover,  $RotD50$  corresponds to the median intensity and was used for the GMMs of the NGA-West2 project (e.g., Boore et al., 2014).

Finally,  $MaxRotD50$  is defined as the median value from the maximum of two orthogonal components for all non-redundant orientations (i.e., over a  $90^\circ$  range). This definition is analogous to  $GMRotD50$  with the geometric mean being changed to the maximum of both orthogonal components. The values of all definitions of Table 1 are represented in Figure 1b for the example ground motion. By definition,  $RotD100$  is always greater than or equal to the rest of the intensities. Moreover, the figure also shows that  $RotD50$ ,  $GM_{AR}$ ,  $GMRotD50$ , and  $GMRotI50$  are very similar to each other, which is usually the case for most ground motions since they all represent measures of central tendency of the intensities from several orientations. Furthermore,  $MaxRotD50$  is between the previous four definitions and  $RotD100$  for the example ground motion, but closer to  $RotD100$ . Finally, the intensity of the arbitrary component has higher variability since it can take the value of a spectral acceleration at any orientation.

## CONVERSION BETWEEN DIFFERENT HORIZONTAL COMPONENTS OF GROUND MOTION

Let  $Y_1$  be a definition of horizontal component with logarithmic mean  $\mu_{\ln(Y_1)}$  and logarithmic standard deviation  $\sigma_{\ln(Y_1)}$  given by a GMM. The logarithmic mean and standard deviation of any other definition of horizontal component  $Y_2$  can be computed using the following equations (Watson-Lamprey and Boore, 2007):

$$\mu_{\ln(Y_2)} = \mu_{\ln(Y_1)} + \mu_{\ln(Y_2/Y_1)} \quad (1)$$

$$\sigma_{\ln(Y_2)}^2 = \sigma_{\ln(Y_1)}^2 + \sigma_{\ln(Y_2/Y_1)}^2 + 2\rho_{\ln(Y_1), \ln(Y_2/Y_1)} \sigma_{\ln(Y_1)} \sigma_{\ln(Y_2/Y_1)} \quad (2)$$

where  $\mu_{\ln(Y_2/Y_1)}$  and  $\sigma_{\ln(Y_2/Y_1)}$  are the logarithmic mean and standard deviation of the  $Y_2/Y_1$  ratio, respectively; and  $\rho_{\ln(Y_1), \ln(Y_2/Y_1)}$  is the correlation coefficient between  $\ln(Y_1)$  and  $\ln(Y_2/Y_1)$ . In this work  $Y_2$  is always  $MaxRotD50$  and the seven remaining definitions listed in Table 1 are used for  $Y_1$ . The three terms required to use Equations (1) and (2), i.e.  $\mu_{\ln(Y_2/Y_1)}$ ,  $\sigma_{\ln(Y_2/Y_1)}$ , and  $\rho_{\ln(Y_1), \ln(Y_2/Y_1)}$ ,

were computed from a ground motion database for the seven different definitions of  $Y_1$ . In order to show the central tendency of the ratios directly, the results of the first term will be presented with an exponential (i.e.,  $\exp(\mu_{\ln(Y_2/Y_1)})$ ), which is equivalent to the geometric mean of the  $Y_2/Y_1$  ratio.

In several cases, the ratio between two horizontal components has a lower and/or upper bound that can be deduced from their definitions (Table 1) or using some idealized ground motion case. The bounds for the ratios considered in this study are summarized in Table 2. The MaxRotD50 to RotD100 ratio cannot exceed 1 since RotD100 is by definition the maximum intensity of any orientation. Moreover, MaxRotD50/RotD50 is greater or equal than 1 since the maximum of two values is always greater than or equal to one of the values. Similarly, the MaxRotD50/GMRotD50 ratio is also always greater than or equal to 1 since the maximum between two values is always greater than or equal to their geometric mean.

**Table 2:** Theoretical limits of the ratios between MaxRotD50 and the rest of the definitions of horizontal ground motion intensity.

Ratio	Lower limit	Upper limit
MaxRotD50 / RotD100	$\cos(22.5^\circ) \approx 0.92^*$	$1^\dagger$
MaxRotD50 / Max <sub>AR</sub>	$\cos(22.5^\circ) \approx 0.92^*$	$\cos(22.5^\circ) / \cos(45^\circ) \approx 1.31^*$
MaxRotD50 / RotD50	$1^\dagger$	$\cos(22.5^\circ) / \cos(45^\circ) \approx 1.31^*$
MaxRotD50 / GMRotD50	$1^\dagger$	$1 / \sqrt{\tan(22.5^\circ)} \approx 1.55^*$
MaxRotD50 / GMRotI50	-	-
MaxRotD50 / GM <sub>AR</sub>	$\cos(22.5^\circ) \approx 0.92^\ddagger$	$\infty^*$
MaxRotD50 / Arbitrary	$\cos(22.5^\circ) \approx 0.92^*$	$\infty^*$

\* Indicates that the limit is derived from the fully polarized case.

† Indicates that the limit is derived directly from the definitions of both components.

‡ Indicates that the limit is derived from a ground motion that is fully polarized and then switches to being fully polarized with the same intensity in an orthogonal orientation.

Most of the bounds shown in Table 2 can be derived from the case of a fully polarized ground motion, where the oscillator responds only in a single orientation that for illustration purposes will be assumed to coincide with one of the as-recorded components. Figure 2 shows the case where the ground motion only occurs in the  $\theta = 0^\circ$  orientation. Spectral accelerations at any other orientation for this fully polarized ground motion are obtained by simple projection, i.e.  $Sa(\theta) = \text{RotD100}|\cos(\theta)|$ . This functional form can be used together with the definitions of Table 1 to compute the values of intensity of this fully polarized ground motion for most definitions of horizontal components, which are also shown in Figure 2. These values can then be used to derive the lower bound of the MaxRotD50/RotD100 ratio and the upper bounds of the MaxRotD50/RotD50 and MaxRotD50/GMRotD50 ratios. Moreover, the lower bound of the MaxRotD50/Arbitrary ratio is found when  $Sa(0^\circ)$  is selected as the Arbitrary component, and no upper bound exists since the Arbitrary component can be zero for  $Sa(90^\circ)$ . The MaxRotD50/GM<sub>AR</sub> ratio also has no upper bound since GM<sub>AR</sub> is zero for the fully polarized case of Figure 2. Furthermore, the lower and upper bounds of the MaxRotD50/Max<sub>AR</sub> ratio also occur for polarized ground motions if the as-recorded orientations are  $\theta = \{0^\circ, 90^\circ\}$  and  $\theta = \{45^\circ, 135^\circ\}$ , respectively.

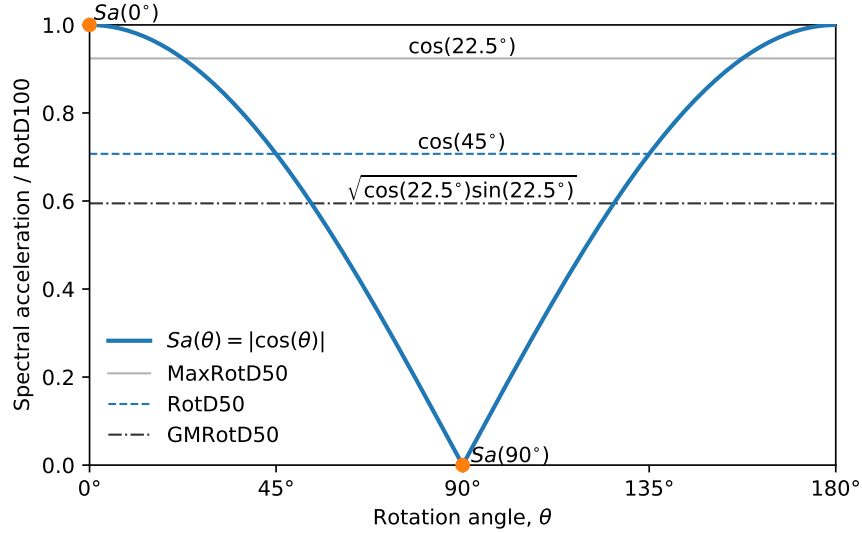


**Figure 2:** Spectral acceleration as a function of rotation angle for a fully polarized ground motion that occurs only in one component ( $\theta = 0^\circ$  in this figure).

An idealized case where the lower bound of the  $\text{MaxRotD50}/\text{GM}_{\text{AR}}$  ratio occurs is when the ground motion is fully polarized in the  $\theta = 0^\circ$  orientation for a portion of the duration of the record and then switches to being fully polarized with the same intensity in the  $\theta = 90^\circ$  orientation. In this case,  $\text{GM}_{\text{AR}}$  would be equal to  $\text{RotD100}$  and  $\text{MaxRotD50}$  would have the same value as the fully polarized case.

No clear bound was found for  $\text{GMRotI50}$  due to its dependence on other periods of the oscillator. Thus, the  $\text{MaxRotD50}/\text{GMRotI50}$  ratio can go beyond the bounds of the  $\text{MaxRotD50}/\text{GMRotD50}$  ratio, although in practice they are very similar.

## GROUND MOTION DATABASE

The ground motions used in this study were obtained from the NGA-West2 database (Ancheta et al., 2014). Only records generated by earthquakes of moment magnitude greater than or equal to 5.0 and recorded in NEHRP site classes B, C, or D were used. Moreover, records “thought to not reasonably reflect free-field conditions” were removed following the procedure used by Boore et al. (2014). These constraints resulted in a total of 5,065 pairs of horizontal ground motion with the distribution of magnitude and Joyner-Boore distance shown in Figure 3.

Spectral accelerations were computed using a critical damping ratio of 5% at 40 periods logarithmically equispaced between 0.01 s and 10 s. Spectral accelerations were only used up to the maximum usable period of the record, which is the inverse of the lowest usable frequency defined by the NGA-West2 database. Thus, the number of records used decrease with increasing period. For example, at a period of 1 s 4996 records are used, whereas at a period of 10 s only 2865 records are used, which corresponds to 57% of the total number of records. The spectral accelerations were computed at rotation angles ( $\theta$ ) from 0 to  $180^\circ$  with  $1^\circ$  increments to compute all the definitions of horizontal component intensity presented in the previous section. This rotation increment of  $1^\circ$  is the same as used in previous studies (e.g., Boore et al., 2006) who found this rotation increment

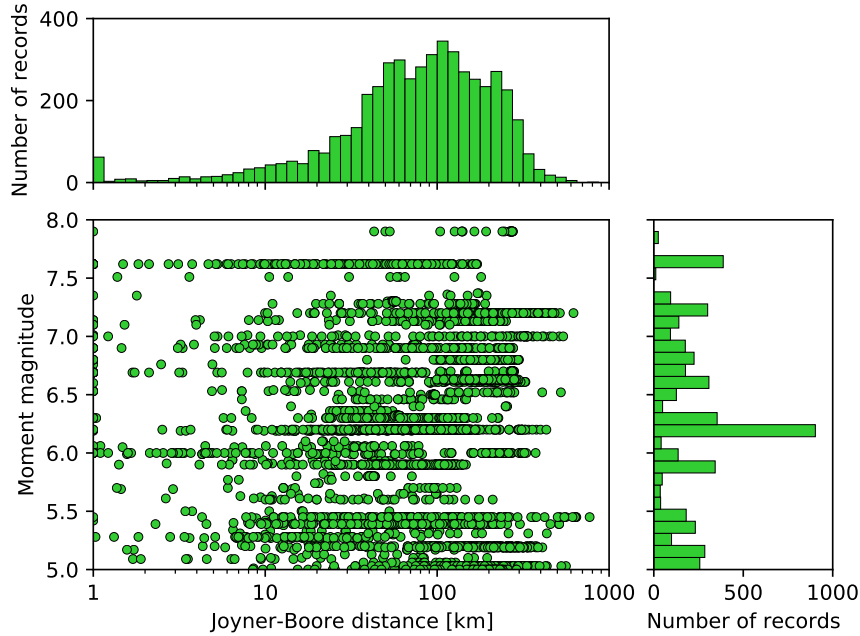


**Figure 3:** Distribution of magnitudes and Joyner-Boore distances of the ground motion records used in the analysis. Records with Joyner-Boore distances lower than 1 km are lumped at 1 km in this figure.

sufficiently small.

## RESULTS

The ratios between MaxRotD50 and six of the other seven definitions of horizontal ground motion intensity are shown in Figure 4 as a function of the structural period for all ground motion pairs in the database. Figure S1 shows the remaining ratio,  $\text{MaxRotD50}/\text{Max}_{\text{AR}}$ , and can be found in the supplemental material to this article. In order to better appreciate the relative values of these ratios, the same limiting values are used in the figure for all ratios. The geometric mean computed for each period is also presented, together with the 16th and 84th percentiles. The ratios of individual records do not follow a trend and can vary significantly from one period to another. However, the geometric mean and percentile curves are more stable and increase with the period for all ratios except  $\text{MaxRotD50}/\text{RotD100}$ , which decreases slightly. Figure 4 also shows that the ratios of all records are within the theoretical bounds presented in Table 2. Apparent “spikes” at very high and very low percentiles (e.g., higher than 95% or lower than 5%) in this figure arise because the period sampling used to compute these ratios for every record is not dense enough to capture the variation with period at these extreme percentiles.

The three expressions required to transform the seven definitions of the horizontal component to MaxRotD50 are presented in Figure 5. The same geometric mean of the different ratios shown in Figure 4 are presented together in Figure 5a. The geometric mean of the  $\text{MaxRotD50}/\text{RotD100}$  ratio is not very sensitive to the periods and has an average value of approximately 0.94. This constant value can be used to estimate MaxRotD50 as a function of RotD100 which is the value

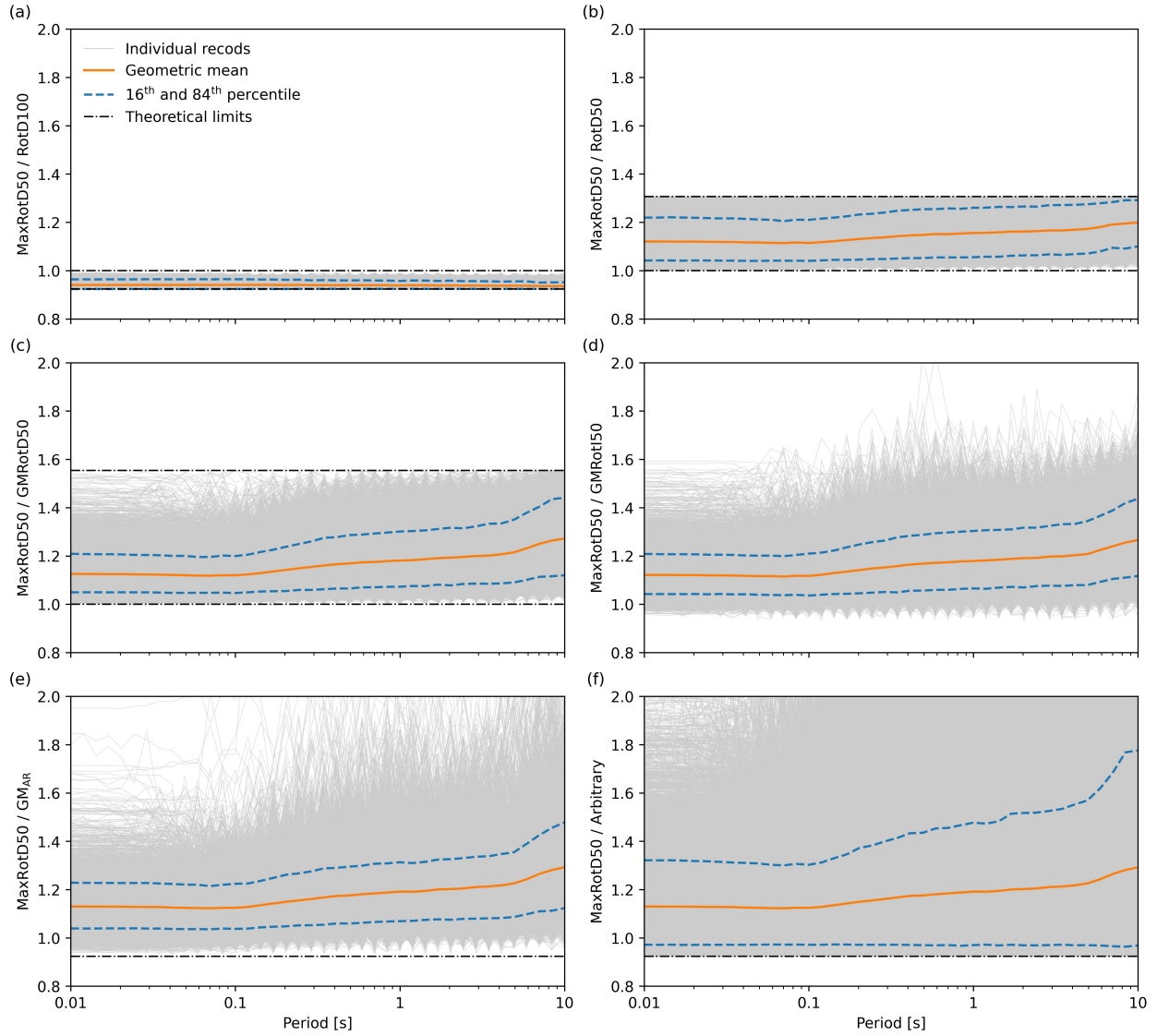


**Figure 4:** Ratios between MaxRotD50 and: (a) RotD100, (b) RotD50, (c) GMRotD50, (d) GM-RotI50, (e) GM<sub>AR</sub>, and (f) Arbitrary. Each gray line represents the ratio from an individual record of the database. Theoretical limits to the ratios are given by horizontal lines. No limits are available for GMRotI50 and the upper limit is infinity for Arbitrary and GM<sub>AR</sub>.

currently used as a basis for design in ASCE 7-16 (American Society of Civil Engineers, 2016). In other words, the use of MaxRotD50 for design would lead to design spectral ordinates approximately 6% lower than those obtained using the maximum intensity. The MaxRotD50/Max<sub>AR</sub> ratio also has a geometric mean that is relatively constant, with its value ranging from 1.01 to 1.02. The geometric means of the rest of the ratios are fairly similar, even though their theoretical limits and record-to-record variabilities vary significantly, as seen in Figure 4. At short periods, the geometric means of these ratios are between 1.12 and 1.13. Starting at 0.1 s the MaxRotD50/RotD50 ratio increases slower than the rest and has a value of 1.2 for a period of 10 s, whereas the rest of the ratios have values ranging from 1.27 to 1.29 for the same period. These differences arise because, at higher periods, displacement time histories tend on average to become more polarized, which leads to RotD50 tending to be greater than the measures that rely on the geometric mean of two components, as seen, for example, in Figure 2. For estimating the geometric mean MaxRotD50/RotD50 ratio, using a constant value equal to 1.12 for periods smaller than 0.1 s and straight-line approximation in semilog axes for periods equal or greater than 0.1 s, that is

$$\frac{\text{MaxRotD50}}{\text{RotD50}} = \begin{cases} 1.12 & T \leq 0.1 \text{ s} \\ 1.155 + 0.0152 \ln(T) & 0.1 \text{ s} < T \leq 10 \text{ s} \end{cases} \quad (3)$$

provides an excellent approximation of this ratio with a coefficient of determination of approximately 0.97.

The second expression required for the transformation is the standard deviation of the natural logarithm of the ratio, which is presented in Figure 5b. The variability of the MaxRotD50 to RotD100 ratio is much lower than the variability of the rest, with a relatively constant standard deviation that ranges from 0.016 to 0.019. The logarithmic standard deviation of the MaxRotD50 to RotD50 ratio is also relatively constant with values of approximately 0.072. Logarithmic standard deviations for the rest of the ratios exhibit a stronger period dependency. The MaxRotD50 to Arbitrary ratio has a much higher logarithmic standard deviation than the rest since its lack of averaging the intensity in various directions results in a significantly larger variability, as shown in Figure 4f.

Finally, the correlation needed in Equation (2) is presented in Figure 5c for all the definitions of horizontal component. All correlations are fairly small with values between -0.15 and 0.2. Correlations where  $Y_1$  is GM<sub>AR</sub>, GMRotI50, GMRotD50, and RotD50 are very similar and always positive, whereas the correlations for RotD100, Arbitrary, and Max<sub>AR</sub> are negative. The numeric values of all curves shown in Figure 5, which are required for the conversions of Equations (1) and (2), can be found in Table S1 (available in the supplemental material to this manuscript).

The evaluation of the influence of the site class, earthquake magnitude, and source-to-site distance on the MaxRotD50/RotD50 ratios is shown in Figure 6. Only the ratios to RotD50 are presented here since it is the most commonly used definition of ground motion intensity in recent GMMs. Figure 6a shows the geometric mean of the MaxRotD50/RotD50 ratio for the three different NEHRP site classes used in this study. The results indicate that there is practically no influence of site class on the ratio of intensities.

The records were also separated into the three one-unit magnitude bins shown in Figure 6b. Although the dependence on magnitude seems to be fairly small, some clear trends can be observed in the figure. For periods smaller than about 4 s, the ratio decreases slightly with increasing earthquake magnitude, whereas the ratio tends to slightly increase with increasing magnitude for periods

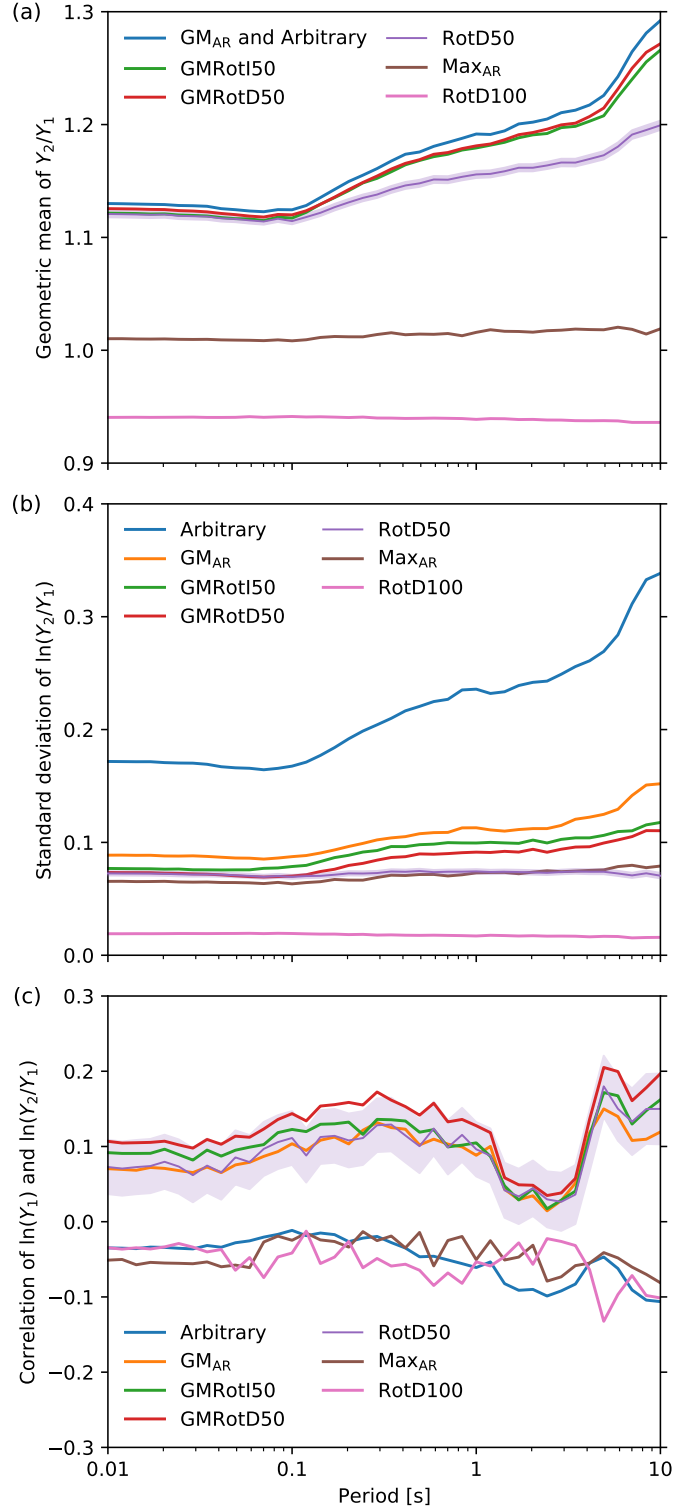


**Figure 5:** Relations required to transform one of the other seven intensities measures ( $Y_1$ ) to MaxRotD50 ( $Y_2$ ): (a) geometric mean of  $Y_2/Y_1$ , (b) standard deviation of  $\ln(Y_2/Y_1)$ , and (c) correlation coefficient between  $\ln(Y_1)$  and  $\ln(Y_2/Y_1)$ . Shaded areas indicate 99% confidence intervals of the relations for RotD50.

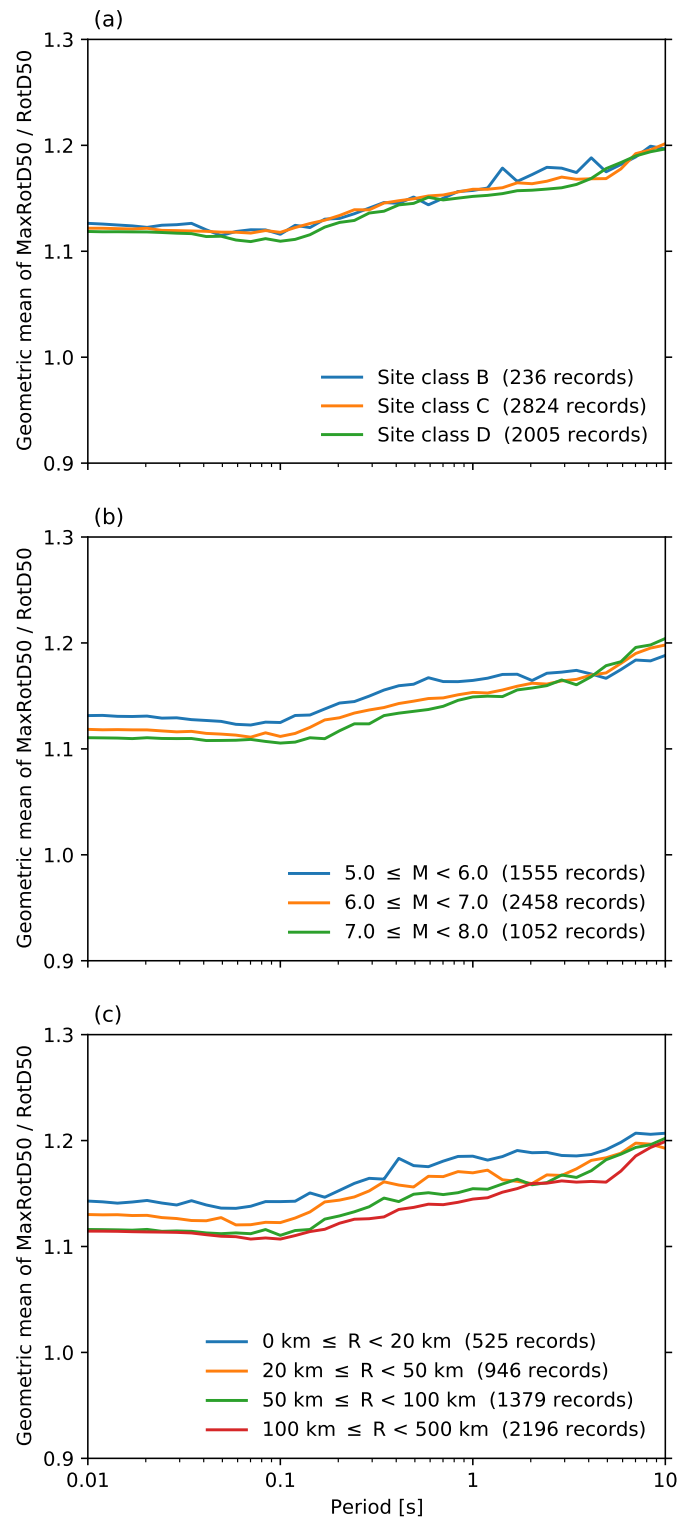


**Figure 6:** Influence of (a) NEHRP site class, (b) moment magnitude, and (c) Joyner-Boore distance on the geometric mean of the MaxRotD50/RotD50 ratio. The number of records in each bin is presented in parentheses.

greater than about 4 s, although this latter trend is less pronounced. These trends of the influence of magnitude are similar to those observed by [Boore and Kishida \(2017\)](#) for the RotD50/GMRot150 and RotD100/RotD50 ratios.

Figure 6c shows the geometric mean MaxRotD50/RotD50 ratio using four bins of Joyner-Boore distance. The ratios tend to decrease with increasing distance. However, at long periods, the influence of distance is less important and smaller than the differences that would arise by using any of the other definitions of the horizontal component shown in Figure 5a. Moreover, the last two distance bins have similar results, suggesting that the distance dependence of the ratios is negligible for distances greater than 50 km. Similar dependencies to those shown in Figure 6 were obtained for the other six definitions of the horizontal component of ground motion and can be found in the supplemental material to this article.

## CONCLUSIONS

This study presents empirically derived period-dependent relations between the recently proposed MaxRotD50 intensity and seven other definitions of horizontal ground motion intensity that have been used previously. The results can be used to transform the logarithmic mean and standard deviation given by a GMM from one of these seven definitions to MaxRotD50. The changes to the logarithmic mean were found to be significant for most definition of horizontal ground motion intensity considered, whereas the changes to the logarithmic standard deviation are very small for all definitions except for the arbitrary component. Thus, neglecting changes to the logarithmic standard deviation seems a reasonable assumption for most engineering applications, although small changes to the standard deviation could impact PSHA results at very high return periods.

Since RotD50 is the most used horizontal component in recent GMMs, special attention was given to its relationship with MaxRotD50. The MaxRotD50/RotD50 ratio was shown to always be greater than 1 and smaller than 1.31. The dependence of this ratio with common inputs of ground motion models was also studied, indicating a negligible dependence on site class and fairly small dependence on earthquake magnitude and Joyner-Boore distance. Similar dependencies on magnitude and distance have also been found for other ratios in previous studies (e.g., [Watson-Lamprey and Boore, 2007](#); [Boore and Kishida, 2017](#)); however, their impact in most engineering applications is very small ([Watson-Lamprey and Boore, 2007](#)). Thus, using directly the values presented in Figure 5, which are independent of the explanatory variables, seems to be a reasonable approximation for the transformation of any of the definitions of horizontal ground-motion intensity used in this study to MaxRotD50.

The relations of this study were obtained using records from shallow crustal earthquakes in active tectonic regimes. Thus, their applicability to other tectonic regimes (e.g., subduction zones and stable continental regions) is still uncertain. However, the results of [Boore and Kishida \(2017\)](#) suggest that these types of ratios are generally similar for different tectonic regimes.

Because most structures have two horizontal principal axes that are orthogonal to each other, rather than designing all structures for the maximum direction intensity (i.e., RotD100) as currently done in ASCE 7-16 ([American Society of Civil Engineers, 2016](#)), a conceptually better approach would be to use MaxRotD50, which would lead to design spectral ordinates approximately 6% lower than RotD100 across all periods. The relations of this study, together with GMMs developed for any of the other seven definitions of horizontal ground motion intensity, can be used to construct

design spectra for MaxRotD50, and then to define amplification factors for RotD100 to be used only for the small percentage of structures that are axisymmetric with cylindrical symmetry with respect to a vertical axis (Stewart et al., 2011; Poulos and Miranda, 2022). Alternatively, the design spectra can be constructed using GMMs developed specifically for MaxRotD50, which could be developed in the future.

## DATA AND RESOURCES

The ground motion records used in this study were obtained from the NGA-West2 ground motion database developed by the Pacific Earthquake Engineering Research Center using the web-based search and download tool (<http://ngawest2.berkeley.edu/spectras/new>, last accessed April 2020). The number of records that can be downloaded at the same time is limited, with the current limit set to 200 records every two weeks. The supplemental material provides the period-dependent expressions required to transform any of the seven definitions of horizontal ground motion intensity considered in this study to MaxRotD50, a figure with the ratios between MaxRotD50 and Max<sub>AR</sub>, and figures with the influence of site class, moment magnitude, and Joyner-Boore distance on the geometric mean ratio between MaxRotD50 and each of the other definitions of horizontal ground motion intensity.

## ACKNOWLEDGMENTS

Financial support to the first author has been provided by the National Agency for Research and Development (ANID) / Doctorado Becas Chile / 2019-72200307. Complementary funding was provided by a seed grant from the UPS foundation to the second author.

## REFERENCES

- Abrahamson, N. A. and W. J. Silva (1997). Empirical response spectral attenuation relations for shallow crustal earthquakes, *Seismol. Res. Lett.* **68**, 94–127.
- American Society of Civil Engineers (2016). *Minimum design loads and associated criteria for buildings and other structures* (ASCE/SEI 7-16 ed.). Reston, VA: American Society of Civil Engineers.
- Ancheta, T. D., R. B. Darragh, J. P. Stewart, E. Seyhan, W. J. Silva, B. S.-J. Chiou, K. E. Wooddell, R. W. Graves, A. R. Kottke, D. M. Boore, et al. (2014). NGA-West2 database, *Earthq. Spectra* **30**, 989–1005.
- Atkinson, G. M. and D. M. Boore (2003). Empirical ground-motion relations for subduction-zone earthquakes and their application to Cascadia and other regions, *Bull. Seismol. Soc. Am.* **93**, 1703–1729.
- Beyer, K. and J. J. Bommer (2006). Relationships between median values and between aleatory variabilities for different definitions of the horizontal component of motion, *Bull. Seismol. Soc. Am.* **96**, 1512–1522.

- Boore, D. M. (2010). Orientation-independent, nongeometric-mean measures of seismic intensity from two horizontal components of motion, *Bull. Seismol. Soc. Am.* **100**, 1830–1835.
- Boore, D. M. and G. M. Atkinson (2008). Ground-motion prediction equations for the average horizontal component of PGA, PGV, and 5%-damped PSA at spectral periods between 0.01 s and 10.0 s, *Earthq. Spectra* **24**, 99–138.
- Boore, D. M., W. B. Joyner, and T. E. Fumal (1997). Equations for estimating horizontal response spectra and peak acceleration from western North American earthquakes: A summary of recent work, *Seismol. Res. Lett.* **68**, 128–153.
- Boore, D. M. and T. Kishida (2017). Relations between some horizontal-component ground-motion intensity measures used in practice, *Bull. Seismol. Soc. Am.* **107**, 334–343.
- Boore, D. M., J. P. Stewart, E. Seyhan, and G. M. Atkinson (2014). NGA-West2 equations for predicting PGA, PGV, and 5% damped PSA for shallow crustal earthquakes, *Earthq. Spectra* **30**, 1057–1085.
- Boore, D. M., J. Watson-Lamprey, and N. A. Abrahamson (2006). Orientation-independent measures of ground motion, *Bull. Seismol. Soc. Am.* **96**, 1502–1511.
- Campbell, K. W. and Y. Bozorgnia (2008). NGA ground motion model for the geometric mean horizontal component of PGA, PGV, PGD and 5% damped linear elastic response spectra for periods ranging from 0.01 to 10 s, *Earthq. Spectra* **24**, 139–171.
- Chiou, B. S.-J. and R. R. Youngs (2008). An NGA model for the average horizontal component of peak ground motion and response spectra, *Earthq. Spectra* **24**, 173–215.
- Hong, H. P. and K. Goda (2007). Orientation-dependent ground-motion measure for seismic-hazard assessment, *Bull. Seismol. Soc. Am.* **97**, 1525–1538.
- Huang, Y.-N., A. S. Whittaker, and N. Luco (2008). Maximum spectral demands in the near-fault region, *Earthquake Spectra* **24**, 319–341.
- Poulos, A. and E. Miranda (2022). Proposal of orientation-independent measure of intensity for earthquake-resistant design, *Earthq. Spectra* **38**, 235–253.
- Sadigh, K., C.-Y. Chang, J. A. Egan, F. Makdisi, and R. R. Youngs (1997). Attenuation relationships for shallow crustal earthquakes based on California strong motion data, *Seismol. Res. Lett.* **68**, 180–189.
- Shahi, S. K. and J. W. Baker (2014). NGA-West2 models for ground motion directionality, *Earthq. Spectra* **30**, 1285–1300.
- Somerville, P. G., N. F. Smith, R. W. Graves, and N. A. Abrahamson (1997). Modification of empirical strong ground motion attenuation relations to include the amplitude and duration effects of rupture directivity, *Seismol. Res. Lett.* **68**, 199–222.

- Stewart, J. P., N. A. Abrahamson, G. M. Atkinson, J. W. Baker, D. M. Boore, Y. Bozorgnia, K. W. Campbell, C. D. Comartin, I. M. Idriss, M. Lew, M. Mehrain, J. P. Moehle, F. Naeim, and T. A. Sabol (2011). Representation of bidirectional ground motions for design spectra in building codes, *Earthq. Spectra* **27**, 927–937.
- Watson-Lamprey, J. A. and D. M. Boore (2007). Beyond  $Sa_{GMRot}$ : Conversion to  $Sa_{Arb}$ ,  $Sa_{SN}$ , and  $Sa_{MaxRot}$ , *Bull. Seismol. Soc. Am.* **97**, 1511–1524.
- Worden, C. B., E. M. Thompson, M. G. Hearne, and D. J. Wald (2020). ShakeMap Manual Online: technical manual, user’s guide, and software guide. <http://usgs.github.io/shakemap> (last accessed November 2020). doi: 10.5066/F7D21VPQ.
- Youngs, R. R., S. M. Day, and J. L. Stevens (1988). Near field ground motions on rock for large subduction earthquakes. In J. L. Von Thun (Ed.), *Earthquake Engineering and Soil Dynamics II — Recent Advances in Ground-Motion Evaluation*, Geotechnical Special Publication No. 20, Park City, Utah, pp. 445–462. American Society of Civil Engineers.